The Structural and Electronic Properties of BaO under Epitaxial Strains: First-Principles Calculations

Xiong Yang*, Ying Wang, Yifei Chen and Huiyu Yan
College of Science, Civil Aviation University of China, Tianjin 300300, China

(Received March 5, 2015; in final form October 10, 2015)

The structural and electronic properties of alkaline-earth oxide BaO under epitaxial strains are investigated using a first principles density functional theory. The electronic structure is particularly sensitive to the compressive or tensile strain, e.g., the splitting of energy band, the increase of the total density of state, and the shift of the partial density of states. Especially, the trends in the variation of the optical band gap are predicted by two different exchange-correlation potential schemes. Our results indicate that the optical band gaps undergo a decrease for both compressive and tensile strains.

DOI: 10.12693/APhysPolA.129.64
PACS: 71.20.Dg, 71.70.Fk, 71.15.Mb

1. Introduction

Among various metal oxides, the alkaline-earth oxide BaO adopts a typical rock-salt structure and has been the subject of many studies [1–3], because of its practical applications. BaO can be applied as a NO_3 storage device for catalysis [1], or as an electrode coating to improve the emission of electrons in cathode ray tubes [2]. As a potential gate dielectric material, BaO is also considered to replace SiO_2 in metal-oxide-semiconductor field-effect transistors (MOSFETs) [3].

It is well known that the applied external pressure or strain can affect the structural and electronic properties of materials significantly, which broadens the opportunities of their technological applications. Indeed, a wide range of corresponding works have been reported [4–8]. For example, the strain-induced structural and electronic property modulations of ZnX (X = O, S, Se, and Te), GdN and XN (X = Al, Ga) have been systematically studied using density functional theory (DFT) [4–7]. Surprisingly, Bousquet et al. predicted theoretically that by applying appropriate epitaxial strains, ferroelectricity can be induced in the alkaline-earth-metal binary oxide such as BaO [8]. Also, they pointed out that the functionalities including the polarization in such strained binary oxides are comparable to those ferroelectric perovskite oxides. This finding motivates our exploration of the physical properties of these compounds under the strains, in order to further explain such phenomena.

In this paper, we intend to investigate the effects of epitaxial strains on the physical and electronic properties of binary oxide BaO by performing an extensive first-principles calculation. Our work may be helpful in better revealing the driving mechanisms of giant ferroelectricity and in devising new applications.

*corresponding author; e-mail: x-yang@cauc.edu.cn

2. Computational method

The calculations in this study are performed within DFT using the plane-wave pseudopotential method [9, 10], as implemented in the Cambridge Serial Total Energy Package (CASTEP) code [11]. The exchange-correlation potential is treated by the generalized gradient approximation (GGA) in the scheme of Perdew–Burke–Ernzerhof (PBE) [12]. The ultrasoft pseudopotential is applied to calculate the electronic structure [13]. The valence electron configurations for the oxygen and barium atoms are considered as $2s^2 2p^4$ and $5s^2 5p^6 6s^2$. A plane-wave cut-off energy of 475 eV and a Monkhorst-pack k-point mesh of $6 \times 6 \times 6$ are required to obtain well-converged results. Geometry optimizations are carried out and convergences are assumed when the forces on atoms are less than 1 meV/Å.

3. Results and discussion

The biaxial strain can be produced by the lattice mismatch, while the equilibrium thin film BaO is epitaxially grown on the substrate with a different lattice constant. The epitaxial strain is defined as $\varepsilon_s = (a - a_0)/a \times 100\%$, where a_0 is the equilibrium lattice constant and a is the strain-induced lattice constant in the {110} plane. For the substrate with a larger (smaller) lattice constant, $\varepsilon_s > 0$ (< 0) corresponding to tensile (compressive) strain. Given a compression or tension, the sufficient relaxation of the lattice parameters a in the {110} plane and c along the [001] axis are performed until the lowest total energy of the fully optimized unit cell is achieved. The calculated structure parameters and unit cell volume for BaO under epitaxial strains are listed in Table I.

It can be seen from the table that our obtained equilibrium lattice parameters and unit cell volume (i.e., under strain-free situations) are in good agreement with the experimental findings of $a = 5.539$ Å and $V = 169.9$ Å^3. By applying the biaxial tensile or compressive stress, the

variations of a, c and V are found to be almost linear. The value of c/a increases (decreases) with compression (tension) increasing, which is consistent with prior work [8].

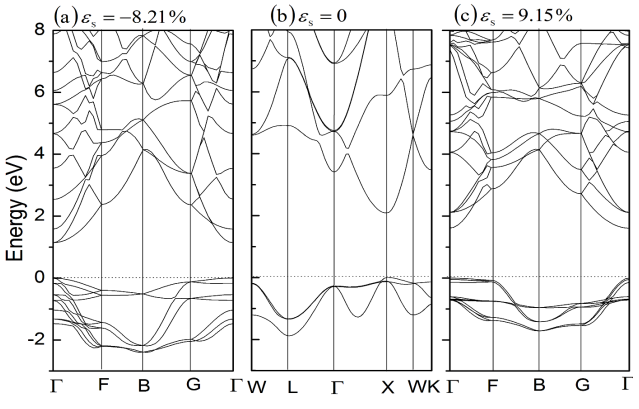

Fig. 1. Electronic band structure for BaO under different strains. The Fermi energy is located at 0 eV, indicated by the dashed line.

Epitaxial strain not only leads to structural transformation, but also triggers the change in the electronic properties. In Fig. 1, we show the effects of the strain on the energy band structure (along high symmetry directions in the Brillouin zone). Figure 1b indicates the band structure of the unstrained BaO at $\varepsilon_s = 0$. Only bands close to the Fermi level are represented. A direct band gap is exhibited between the valence-band maximum and conduction-band minimum at high-symmetry point X (0.5, 0.0, 0.5). Our obtained band gap is 2.08 eV, which is in accordance with the calculated result of 2.0 eV using a full-potential linear augmented plane-wave plus local-orbital method and GGA [14], and slightly larger than the local density approximation (LDA) result of 1.75 eV [15]. Compared to the experimental value of 4.8 eV [16], the theoretical values reflect the well-known problem that GGA or LDA method usually underestimates the band gap. Although it has been suggested in Refs. [7, 17, and 18] that the GW approximation or hybrid functional theory can improve the theoretical values of the band gap, the calculations using GW theory or hybrid functional theory are more sophisticated than the DFT–GGA method. In a word it is usually accepted that this error can be roughly compensated by an appropriate shift of the conduction bands, and a simple GGA calculation can predict quite reliably main characters of the band structure and the trends in the dependence of the band gap on epitaxial trains [4–6].

TABLE I

Calculated structure parameters of BaO under epitaxial strains.

ε_s[%]	–5.42	–4.47	–3.40	–2.41	–1.31	0	1.14	2.52	3.63	4.67	5.74
a [Å]	5.291	5.344	5.404	5.459	5.521	5.594	5.658	5.735	5.797	5.855	5.915
c [Å]	5.816	5.772	5.725	5.685	5.641	5.594	5.555	5.511	5.478	5.449	5.421
V [Å^3]	162.8	164.9	167.2	169.4	172.0	175.1	177.8	181.3	184.1	186.8	189.7

We present the band structures of BaO at epitaxial strains of -8.21% and 9.15% in Fig. 1a and c. Under the {110} plane strain, the lattice symmetry is lowered to the tetragonal one and the space group changes from $Fm3m$ to $I4/mmm$. Therefore, the high symmetry directions of the Brillouin zone change as the shape of Brillouin zone changes. The selected high symmetry points on the abscissa in Figs. 1a and c are different from that in Fig. 1b. Obviously, the electronic band structures are particularly sensitive to lattice strains. Compared to the equilibrium electronic structure, several interesting observations here can be made: (1) Under the conditions of strains, BaO still displays a direct gap, but at the high symmetry point Γ (0, 0, 0). (2) The conduction band states are shifted towards lower energies by the compression or tension, i.e., the optical band gap becomes smaller. (3) The degenerated valence and conduction bands in the cubic phase are split now, i.e., more eigenvalues distribute among k points in the Brillouin zone, because a compression or tension reduces the lattice structure to a tetragonal phase. Spin–orbit couplings (not considered in this calculation) might introduce further splitting.

The total and partial density of states for the strain-free BaO are shown in Fig. 2. The top of the valence band has mostly O $2p$ character, while the bottom of the conduction band is determined by Ba $4d$ electrons. The main features of the occupied and unoccupied O $2p$ densities of states match quite well with the measurements of X-ray emission spectroscopy (XES) and X-ray absorption spectroscopy (XAS) as well as previous calculations [14]. There are visible O $2s$–Ba $5p$ hybridizations in the lower energy region around 11.5 eV and 15 eV, respectively, with small amount of Ba $4d$ states mixed in. The O $2p$ electronic states hybridize with Ba sd states in both the upper valence bands and the conduction bands.

The density of states are also modified by the epitaxial strain, as plotted in Figs. 3 and 4. Comparing Figs. 3a and 4a with Fig. 2a, the total density of state increases more than 50% when the compressive (tensile) strain on the lattice constant attains to -8.21% (9.15%). This implies that the O $2p$–Ba $4d$ hybridization becomes stronger, which will result in anomalous Born effective charge as an important feature for ferroelectricity [8, 19]. According to the partial density of states in Figs. 2–4, it

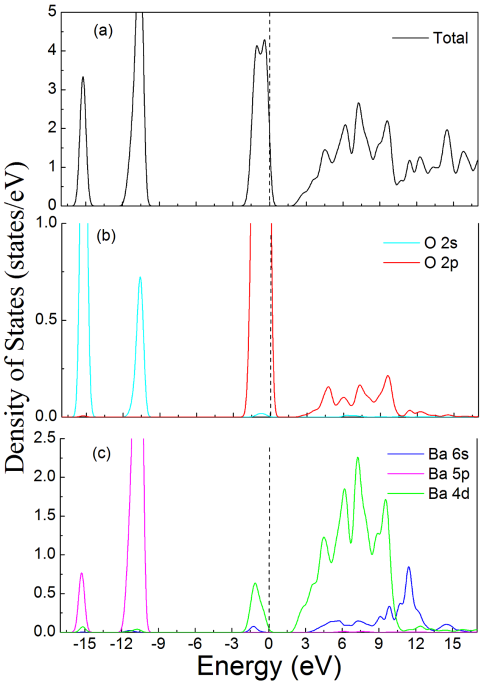

Fig. 2. Total and partial density of states for the equilibrium BaO. The Fermi energy is located at 0 eV, indicated by the dashed line.

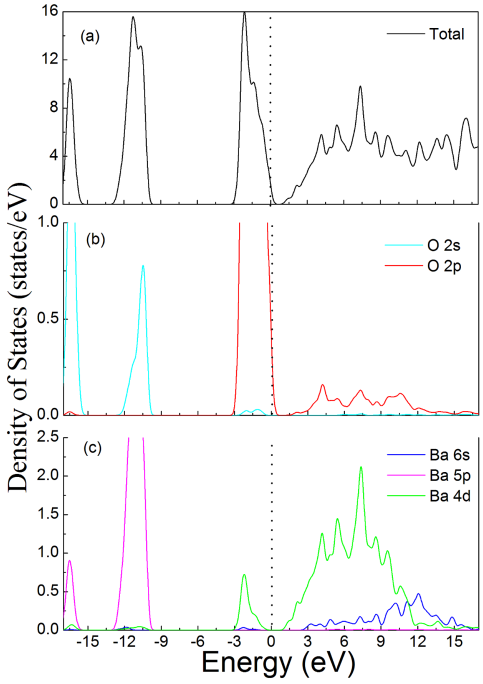

Fig. 3. Total and partial density of states for BaO under the compressive strain of $\varepsilon_S = -8.21\%$.

is clear that the O $2p$ and Ba $4d$ states in the bottom of the conduction band have obvious shifts towards the Fermi energy, because of the effect of the compressive or tensile strain. This is the physical reason for the reduction of the band gap, which can be also found from the total density of states in Figs. 2a–4a.

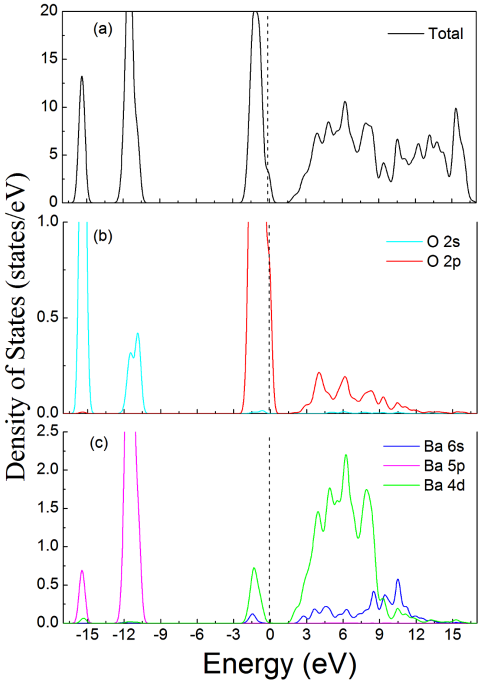

Fig. 4. Total and partial density of states for BaO under the tensile strain of $\varepsilon_S = 9.15\%$.

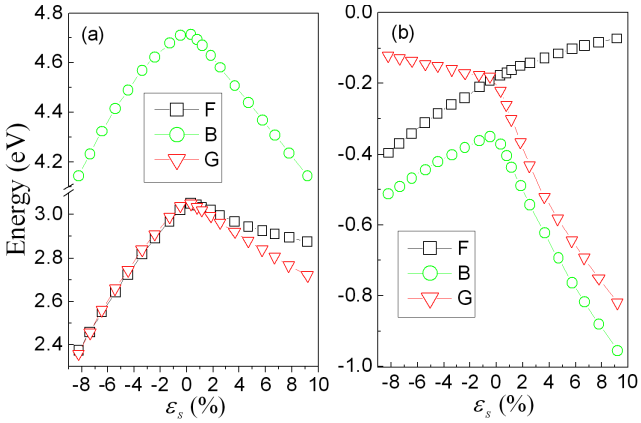

Fig. 5. (a) The minima of the conduction states and (b) the maxima of the valence states at different high symmetry points for BaO under the epitaxial strains of ε_S.

In order to better reveal the mechanisms of the energy band structure, Fig. 5 indicates the minima of the conduction states (CBMs) and the maxima of the valence states (VBMs) at the high symmetry points, as a function of the strain ε_S. In Fig. 5a, the CBMs at the F, B, and G points decrease with the increase of the compressive or tensile strain, especially the F and G states with very close energies share the similar trends. This is attributed to that the F and G states are dominated by the Ba $4d$ electrons. The O $2p$ electronic states and Ba $6s$ states provide much contribution to the energy of the B point, which results in the B energy being larger than the F and G energies in the whole of ε_S

range. For the valence bands shown in Fig. 5b, the F and G points in energy exhibit opposite trends for two types of strains. As the compressive (tensile) strain increases, the F energy decreases (increases). The B energy always decreases with compression or tension increasing. This is due to the change of the O and Ba electronic states near the Fermi energy under strains.

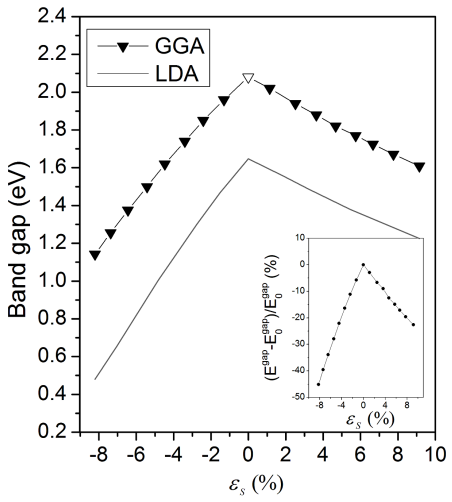

Fig. 6. Band gap (E^{gap}) as a function of ε_{S} for BaO, applying the GGA (with symbol) and the LDA (without symbols). The equilibrium band gap (E_0^{gap}) is indicated by open symbol. Inset shows the corresponding relative variation of the GGA band gap.

The energy band gap is arguably one of the most important parameters in materials, and it is necessary to study the band gap modulations under strains in order to tailor materials for use in specific devices. The strain-induced variation of the band gap for BaO is shown in Fig. 6. Our results indicate that the maximum value of the band gap occurs at strain-free equilibrium. Both biaxial tensile and compressive strains result in a notable narrowing of the band gap, which is due to enhanced orbital coupling between cation and anion atoms. The similar feature can be found in the zinc blende phase of ZnX systems in Ref. [4]. The band gap E^{gap} of BaO decreases linearly as $E^{\mathrm{gap}} = 0.11\varepsilon_{\mathrm{S}}+2.08$ with compression, $E^{\mathrm{gap}} = -0.05\varepsilon_{\mathrm{S}} + 2.08$ with tension, respectively. As a result, the interband transition of an electron from the valence band to the empty states of the conduction band needs less energy. The redshift of absorption edge for BaO under the strain will be observed in the experiment. The inset of Fig. 6 also shows the relative variation in the GGA band gap with respect to the equilibrium value as a function of ε_{S}. It can be seen that for $-8.2\% < \varepsilon_{\mathrm{S}} < 0$ (under compression), the band gap decreases by approximately 45%, while for $0 < \varepsilon_{\mathrm{S}} < 9.2\%$ (under tension), it undergoes a reduction by about 22%.

To examine the accuracy of our calculations, the trends in the variation of the band gap values calculated by the LDA are plotted in Fig. 6. Obviously, the predictions given by the GGA and the LDA are in qualitative agreement with each other. That is to say, the specific choice of the exchange correlation functional appears not to change the trends of the band gap variation. The exact band gap value at any particular strain might not be precisely determined from DFT-based calculations. However, the trends are clear, and the predicted changes could be observed in experiment.

Bousquet et al. demonstrated that ferroelectricity can be engineered in different alkaline-earth-metal oxides by using epitaxial strains [8]. They reported that for BaO at strains of $\varepsilon_{\mathrm{S}} = -2.66\%$ and 3.03%, the polarizations (P) are 29 μC/cm^2 and 21 μC/cm^2, respectively, which are comparable in amplitude to a typical ferroelectric perovskite oxide such as $BaTiO_3$ ($P = 34$ μC/cm^2). According to our theoretical calculations shown in Fig. 6, we can estimate that the actual band gaps of BaO at strains of $\varepsilon_{\mathrm{S}} = -2.66\%$ and 3.03% are about 4.51 eV and 4.65 eV, respectively, with respect to the equilibrium experimental gap 4.8 eV. These values are larger than the band gap 3.0 eV of $BaTiO_3$. Therefore, the strained BaO may be an attractive candidate to replace ferroelectric perovskite $BaTiO_3$ as possible gate dielectric for MOSFET transistor, due to that a small band gap will result in unsuitable band offsets with Si more easily [20].

4. Conclusion

In summary, we have reported first-principles calculations of strain-induced physical and electronic structure changes in BaO, as an example of alkaline earth oxide. The effects of the compressive and tensile strains on the structure, energy band and density of states are originally predicted. The most important effect is the variation in the band gap. The consistent predictions obtained by GGA and LDA are that both compressive and tensile strains result in reductions of the band gap, which may be a response to the experimentally observed redshift of the absorption edge. Our calculations of the band gap provide a theoretical basis that BaO under appropriate strain is an attractive candidate as possible gate dielectric for MOSFET transistor.

Acknowledgments

This work was supported by the Scientific Research Foundation of Civil Aviation University of China (No. 09QD10X), by the Fundamental Research Funds for the Central Universities (3122014K003).

References

[1] N.W. Cant, M.J. Patterson, *Catal. Today* **73**, 271 (2002).

[2] K.C. Mishra, R. Garner, P.C. Schmidt, *J. Appl. Phys.* **95**, 3069 (2004).

[3] K.J. Hubbard, D.G. Schlom, *J. Mater. Res.* **11**, 2757 (1996).

[4] S.K. Yadav, T. Sadowski, R. Ramprasad, *Phys. Rev. B* **81**, 144120 (2010).

[5] H.M. Liu, C.Y. Ma, C. Zhu, J.M. Liu, *J. Phys. Condens. Matter* **23**, 245901 (2011).

[6] L. Dong, S.K. Yadav, R. Ramprasad, S.P. Alpay, *Appl. Phys. Lett.* **96**, 202106 (2010).

[7] L. Qin, Y. Duan, H. Shi, L. Shi, G. Tang, *J. Phys. Condens. Matter* **25**, 045801 (2013).

[8] E. Bousquet, N.A. Spaldin, P. Ghosez, *Phys. Rev. Lett.* **104**, 037601 (2010).

[9] P. Hohenberg, W. Kohn, *Phys. Rev.* **136**, B864 (1964).

[10] W. Kohn, L.J. Sham, *Phys. Rev.* **140**, A1133 (1965).

[11] V. Milman, B. Winkler, J.A. White, C.J. Packard, M.C. Payne, E.V. Akhmatskaya, R.H. Nobes, *Int. J. Quantum Chem.* **77**, 895 (2000).

[12] J.P. Perdew, K. Burke, M. Ernzerhof, *Phys. Rev. Lett.* **77**, 3865 (1996).

[13] D. Vanderbilt, *Phys. Rev. B* **41**, 7892 (1990).

[14] J.A. McLeod, R.G. Wilks, N.A. Skorikow, L.D. Finkelstein, M. Abu-Samak, E.Z. Kurmaev, A. Moewes, *Phys. Rev. B* **81**, 245123 (2010).

[15] J. Junquera, M. Zimmer, P. Ordejón, P. Ghosez, *Phys. Rev. B* **67**, 155327 (2003).

[16] W.H. Strewlow, E.L. Cook, *J. Phys. Chem. Ref. Data* **2**, 163 (1973).

[17] U. Schönberger, F. Aryasetiawan, *Phys. Rev. B* **52**, 8788 (1995).

[18] E.L. Shirley, *Phys. Rev. B* **58**, 9579 (1998).

[19] P. Ghosez, J.-P. Michenaud, X. Gonze, *Phys. Rev. B* **58**, 6224 (1998).

[20] J. Junquera, P. Ghosez, *J. Comput. Theor. Nanosci.* **5**, 2071 (2008).